

Thin Film Deposition & Vacuum Technology

THIN FILM DEPOSITION & VACUUM TECHNOLOGY

By
Stefan Cannon Lofgran

A senior thesis submitted to the faculty of
Brigham Young University–Idaho
in partial fulfillment of the requirements for the degree of

Bachelor of Science

Department of Physics
Brigham Young University–Idaho
April 2013

2013 © Stefan Lofgran
All Rights Reserved

Brigham Young University–Idaho

Department Approval

of a senior thesis submitted by
Stefan Cannon Lofgran

This thesis has been reviewed by the research committee, senior thesis coordinator and department chair and has been found to be satisfactory.

Date

David Oliphant, Advisor

Date

Ryan Nielson, Committee Member

Date

Stephen McNeil, Senior Thesis Coordinator

ABSTRACT

THIN FILM DEPOSITION & VACUUM TECHNOLOGY

Stefan Cannon Lofgran
Department of Physics
Bachelor of Science

The study and development of thin films via physical vapor deposition has played a significant role in the development of optical coatings, semiconductors, and solar cells. Closely related to the study of thin films is the development of vacuum technology and systems capable of reaching pressures suitable for growing uniform films at reasonable deposition rates. This paper explores the method of physical vapor deposition known as thermal evaporation via resistive or Joule heating as a means for growing thin aluminum (Al) films on a mineral glass substrate. Methods for measuring thickness are also discussed and investigated in an attempt to determine the experimentally produced film thickness. A detailed explanation of the development and operation of the vacuum system in which the Al films were grown is given as well as future improvements that could be made.

ACKNOWLEDGEMENTS

To my loving wife & family who have supported me the whole way, and to David Oliphant who has guided me on this project.

Table of Contents

	Page
Abstract	iii
Acknowledgements	iv
List of Figures	vii
List of Tables	viii
1 Introduction	1
1.1 A Brief History of Thin Film & Vacuum Technology	1
1.2 Review of Theory	4
2 Experimental Design & Setup	9
2.1 Vacuum System Design	9
2.1.1 Recent Developments	9
2.1.2 Using a Viton Gasket	10
2.1.3 Vacuum Conditioning	12
2.2 Deposition System Design	14
2.2.1 The Original Experiment	14
2.2.2 New Crucibles & Improved Temperature Calculations	15
2.2.3 Power Supplies & Feedthroughs	17
2.2.4 Substrate Holder Design	18
3 Procedures & Documentation	21
3.1 Equipment Documentation	21
3.1.1 Silicon Heating Tape	21
3.1.2 Type C Thermocouple	22
3.1.3 Quartz Crystal Microbalance	23
3.1.4 Residual Gas Analyzer	24
3.1.5 Crucibles, Baskets, & Boats	25

3.1.6	Power Supplies	25
3.2	Vacuum Procedures	26
3.2.1	Pumping to Low Vacuum	26
3.2.2	Pumping to High Vacuum	27
3.3	Deposition Procedure	28
4	Thin Film Deposition Rates	29
4.1	Initial Rate Calculations	29
4.2	Effects of Slide Outgassing	31
5	Future Experiments & Summary	35
5.1	Improving Film Quality	35
5.2	Improved Deposition Rates	36
	Bibliography	38
	Appendix A	40
	Appendix B	42
	Appendix C	45
	Appendix D	49
	Appendix E	50
	Appendix F	53

List of Figures

1.1	RGA cracking patterns	5
1.2	Langmuire-Knudsen angle dependence	6
1.3	Initial deposition system configuration	7
2.1	BYU-Idaho Vacuum system	10
2.2	25" OD CF Flange	11
2.3	O-ring over compression failure	12
2.4	RGA P vs T graph	14
2.5	Various boats and baskets [1]	15
2.6	Broken tungsten baskets	16
2.7	Broken quartz crucibles	17
2.8	New crucible holder configuration	18
2.9	Old crucible configuration	19
2.10	Substrate holder design	20
3.1	Quartz Crystal Microbalance Positioning	24
3.2	Crucible & basket combination	25
4.1	Filmed slide projection	30
4.2	Average change in slide mass over time	33
4.3	Change in slide mass between consecutive days	34

List of Tables

1.1	Vacuum quality pressure ranges	2
3.1	Silicon Heat Tape Specifications	22
3.2	Type C thermocouple specifications	23
3.3	Genesys 60-12.5 power supply details	26

Chapter 1

Introduction

1.1 A Brief History of Thin Film & Vacuum Technology

Vacuum technology is becoming increasingly important within physics due to its several applications. The ideal vacuum is a space devoid of all particles. All vacuum systems aren't created equal, and like many things in physics actual vacuum systems fall short of the ideal. The base pressure a system maintains determines the quality of its vacuum. These levels aren't strictly defined, but are generally described as rough, low, medium, high, or ultra high (see Table 1.1). The most obvious factors determining the type of vacuum achieved are the equipment used and the system configuration. Before delving into the details of vacuum design and its importance in developing thin films it will be beneficial to review a brief history of how vacuum systems were first developed.

One of the first contributors to vacuum technology was Otto von Guericke. Von Guericke developed the first vacuum pump sometime in the 1650's[2]. With his pump, he was able to study some of the most basic properties of vacuums. Von Guericke believed that his pump pulled the air out of a container, which is actually incorrect. Vacuum pumps cannot pull the gases out of a container rather they

Vacuum Type	Pressure Range (Torr)
Low	760 - 0
Medium	0 - 10^{-3}
High	10^{-3} - 10^{-8}
Ultra High	10^{-8} - 10^{-12}
Extreme High	$< 10^{-12}$
Outer Space	$\sim 10^{-16}$

Table 1.1: Vacuum quality pressure ranges

create a difference in pressure which causes the gas in the high-pressure area to move to the low-pressure area. Essentially, a vacuum pump generates a vacuum by creating pressure differences, which creates a flow of gas that exits the chamber at a rate faster than the rate at which gas enters the chamber.

Aside from Von Guericke, there were several other contributors to what is now considered modern vacuum technology. Many of these individuals lived before or during the same time as Otto von Guericke. Evangelista Torricelli, the man who the unit of pressure Torr is named after, was one of the first to recognize a sustained vacuum while observing mercury in a long tube. He noted his discovery, but never actually published his findings because he was more interested in mathematics. Hendrik Lorentz, Blaise Pascal, Christiaan Huygens, and others all played crucial roles in defining and developing the fundamental principles upon which modern vacuum systems run.

Modern vacuum technology is constantly adapting to be used in a broader range of applications in a plethora of disciplines within physics and engineering, such as vacuum packaging, welding, and electron microscopes. Even though vacuum technology has developed rapidly since the 1600's, what most would define as modern vacuum technology isn't that old. Scientists and engineers developed most of the technology that we use today during and after World War II. During the

period of development after World War II people began to revisit thin films and explore the possibilities of their uses in industry, particularly in the semiconductor industry.

One of the most important applications of vacuum systems is the development of thin films. Physical vapor deposition (PVD) is just one method of producing thin films. Michael Faraday pioneered the first PVD process in the early 1800's [1]. Many sub processes fall under the description of PVD including electron beam, sputtering, thermal, and plasma arc deposition methods. At BYU-Idaho the method used to produce thin films is a thermal evaporative deposition. Thermal evaporation deposition is the most basic method used to produce thin films. The first use of the term PVD was used in C. F. Powell, J. H. Oxley, and J. M. Blocher Jr.'s book Vacuum Coatings in 1966 [3]. They were not the first to use PVD methods for developing thin coatings either, but their text helped to establish and clarify the PVD processes that were known by that time. Since Powell, Oxley, and Blocher's publication scientists have devised many new methods for growing films. Recent developments in the past few decades have produced methods capable of growing alloy films and processes suitable for large scale production in order to better meet the demands of consumers.

Today's society overlooks the importance of vacuum coatings in products they use. The semiconductor industry relies heavily on thin film technology to produce flash memory and computer chips. Companies developing optical products often use optical polarizers and beam splitters in their designs. Other industries also use thin film technology most of which is for cosmetic purposes, such as mirrors and toys.

1.2 Review of Theory

At this point an in depth exploration of gas flow regimes will not be discussed, but if the reader is interested they would benefit greatly from reading O’Hanlon’s *A User’s Guide to Vacuum Technology* [4]. Film quality and vacuum system pressure are inseparably connected. Uniformity and purity are the main elements in determining a film’s quality. Uniformity is an issue that was not addressed during the development of the BYU-Idaho deposition system. Getting the system to function properly is a prerequisite to tasks concerning the film uniformity. The purity of the material prior to deposition is the largest factor in determining the films purity. The second biggest factor is most likely the gas composition and pressure of the system in which the film was developed. Vacuum technicians know that these two elements of a vacuum system are difficult to control. At BYU-Idaho, we focus on trying to analyze these factors rather than control them at the present time. To analyze the gas composition in our vacuum system we rely on a 200 AMU residual gas analyzer (RGA). The RGA is a quadrapole mass spectrometer that can determine the atomic mass of gas molecules in a system by ionizing the particles and measuring the change in voltage of an electrode when the ionized gas collides with it. The RGA uses the voltages to then produce cracking patterns used to determine the gas composition of the chamber (see figure 1.1).

A substantially low pressure is required to prevent film oxidation and reduce the contaminant density. A pressure of 10^{-5} Torr is sufficient, but lower pressures would help reduce the density of contaminants in the film. At 10^{-5} Torr the mean free path of gas in the chamber is approximately 8 meters, which without the unit of measurement is often referred to as the Knudsen number. The mean free path can

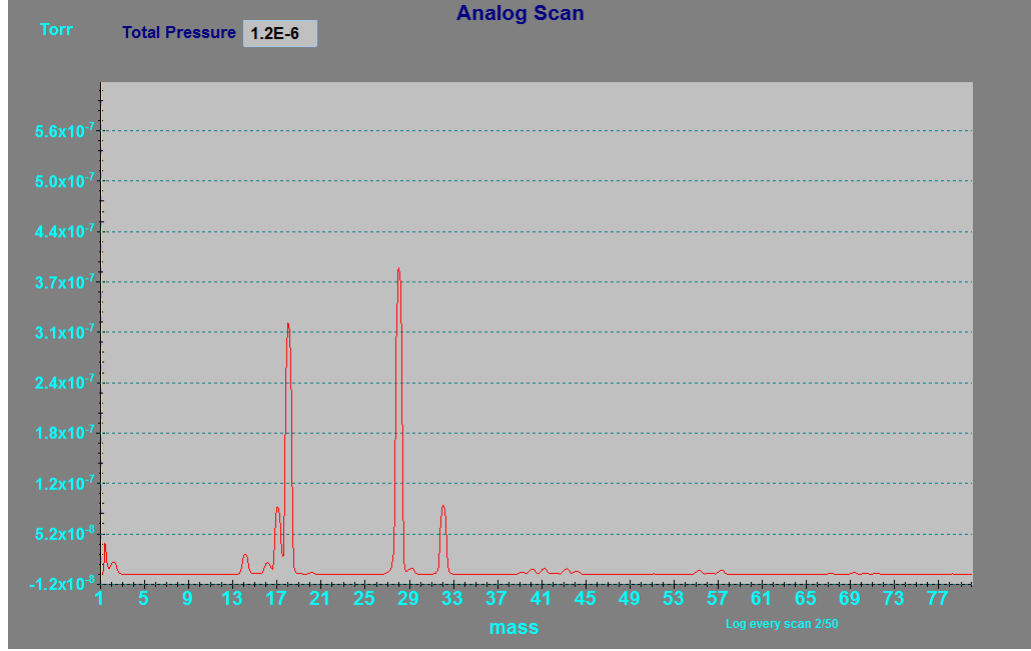


Figure 1.1: RGA cracking patterns

be calculated using the following equation

$$l = \frac{k_B T}{\sqrt{2} \pi d^2 P}, \quad (1.1)$$

where k_B is the Boltzman constant, T is the temperature in Kelvin, d is the diameter of the molecule in meters, and P is the pressure in Pascals. As the mean free path of the gas particles increases, so does the Knudsen number. When the Knudsen number is close to or greater than one, gas particles obey principles of free molecular flow more than viscous flow. The Langmuire-Knudsen equation is founded on the assumption that the molecules follow a molecular flow regime. The Langmuire-Knudsen equation is

$$R_m = C_m \sqrt{\frac{M}{T}} \cos \theta \sin \phi \frac{1}{r^2} (P_e(T) - P), \quad (1.2)$$

where R_m is the rate per unit area of the source, $C_m = 1.85 \times 10^{-2} \frac{\text{mol} \cdot \text{K}}{\text{s} \cdot \text{Torr}}$ a constant, M is the gram-molecular mass of the deposition material, T is the temperature of

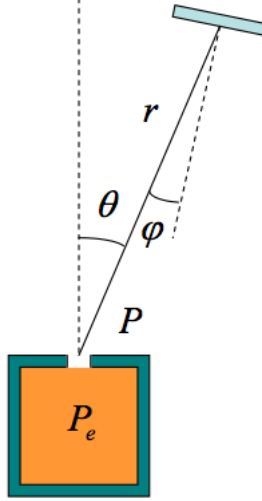


Figure 1.2: Langmuire-Knudsen angle dependence

the deposition material, θ is the angle between the normal of the source and the substrate, ϕ is the angle normal to the surface of the substrate and crucible, r is the distance between the crucible and substrate, and P and P_e are the system pressure and evaporant partial pressure in Torr respectively. Another assumption of the Langmuire-Knudsen equation is that the evaporant molecules will travel from the crucible where they are heated to the substrate without “picking” up any other gas particles in the chamber (see figure 1.2). Subsequently, a decrease in the base pressure of the vacuum will also reduce the number of particles “picked” up as they flow towards the substrate to be deposited.

The Langmuire-Knudsen equation necessitates the use of other methods and equations to calculate an accurate deposition rate. Among these is Stefan-Boltzman equation for blackbody radiation:

$$\mathcal{P} = IV = \sigma \epsilon AT^4, \quad (1.3)$$

where \mathcal{P} is the electrical power through the crucible, I is the current, V is the voltage, σ is the Stefan-Boltzman constant, ϵ is the emissivity, A is the surface area

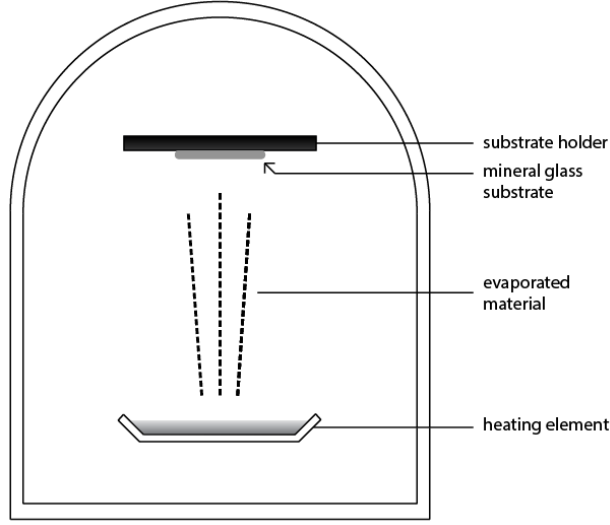


Figure 1.3: Initial deposition system configuration

of the black body, and T is the temperature. Solving for T we find

$$T = \left[\frac{IV}{\sigma \epsilon A} \right]^{\frac{1}{4}}. \quad (1.4)$$

I also used an experimentally derived equation for determining the partial pressure of liquid Al[5] given by

$$\log P = -\frac{15993}{T} + 12.409 - 0.999 \log T - 3.52 \times 10^{-6}T, \quad (1.5)$$

where P is the pressure in Torr and T is the temperature. There are, of course, many other methods capable of deriving the necessary quantities. At the time of the initial experiment, these were the best approximations available to us, but with the addition of a type C thermocouple, new vacuum feedthrough, and power supply; our capability to derive the temperature more accurately has improved. Feasible alternatives to approximating the crucible temperature solely by using a blackbody approximation include incorporating power loss/transmission calculations and the use of a thermocouple.

Understanding the fundamentals of vacuum theory can prevent many of the complications that diminish the accuracy and precision of collected data. Recognizing the sources of leaks in a vacuum system is one item that is of particular interest for experimentalists. A variety of sources lead to unwanted gas added to the chamber by leaks. Vacuum leaks are often due to the pressure gradient that exists within a vacuum, which creates a surplus of interesting and inimical problems. Thus vacuum leaks should be addressed prior to experimentation. At a standard temperature and pressure, almost everything absorbs water vapor and other gases. One factor that affects how much water vapor is absorbed by a material is the humidity. Inside a vacuum, these materials release the gases they absorbed because the same forces that helped trap gasses in them have diminished. As a result, preparing materials prior to use inside the chamber and considering their impact on the data is an important step in the experimental process.

All materials will experience some outgassing within a vacuum chamber. A judicious selection of materials will reduce the effects of outgassing, or leaking of gas, from materials that are used. For this reason, conditioning of the vacuum chamber and, if possible, all the materials used in the chamber is also an important step of experimentation. Chemical cleaning or pre-exposure to vacuum pressures are both ways to condition materials for use in vacuum. More technical processes such as those used in developing semiconductors have prescribed standard methods for cleaning materials prior to use in vacuum.

Chapter 2

Experimental Design & Setup

2.1 Vacuum System Design

2.1.1 Recent Developments

BYU-Idaho purchased the vacuum chamber, pressure gauges, roughing pump, and residual gas analyzer; but received the oil diffusion pump and gate valve as a donation from another university. The important details about almost all of the equipment are known. However, we don't know the material or manufacturer of the O-ring used with the chamber.

Within the past year, improvements to the vacuum system have helped to achieve lower pressures more consistently. Initially, the BYU-Idaho vacuum chamber operated with only a couple thermocouple pressure gauges, ion pressure gauge, oil diffusion pump backed by a rotary vane roughing pump, viewport, RGA, and single high voltage electrical feedthrough (The current design can be seen in figure 2.1). While these are sufficient to achieve pressures suitable for PVD, there is always room for improvement.

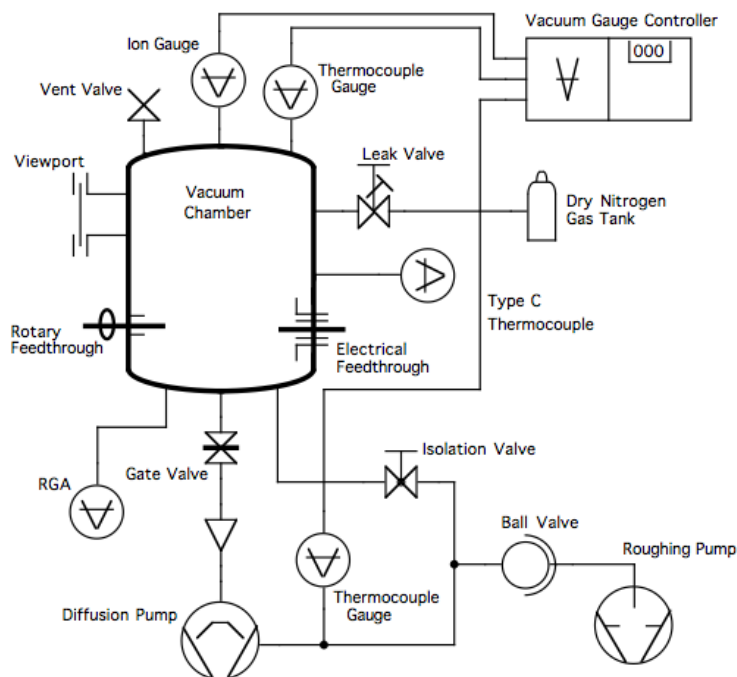


Figure 2.1: BYU-Idaho Vacuum system

The goal that drives development of the vacuum system is that of achieving the lowest base pressure possible. It is far more difficult to achieve an ultra-high vacuum than it is to reach a low vacuum. Fortunately, the oil diffusion pump that is used has a very high throughput rate of about 2,000 L/s. This makes it possible to achieve pressures as low as 10^{-8} Torr with the current pump configuration. Despite this advantage, other elements of the system do more to limit the achievable pressure than the pump.

2.1.2 Using a Viton Gasket

A pitfall of the current design is lack of smaller ports to transfer materials in and out of the chamber. The system has a cylindrical design with feedthrough ports along the sidewall and the chamber separates above the feedthroughs with a 25" outer diameter (OD) conflat flange (CF) (this can be seen in figure 2.2). The Viton

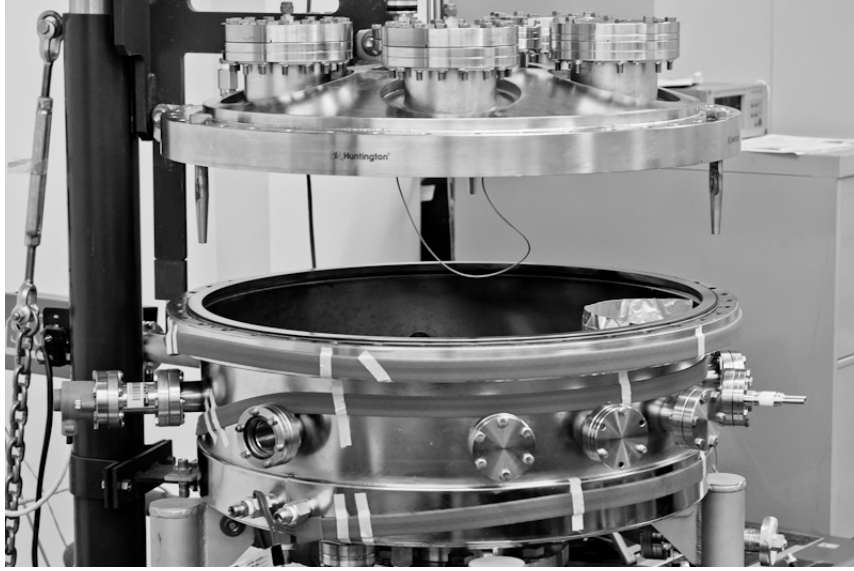


Figure 2.2: 25" OD CF Flange

O-ring that is used, however, makes this flange a possible source of significant leaking. If a metal gasket and the securing bolts were used this flange wouldn't be a big problem.

In order to moderate the side-effects of using a large Viton gasket it must fit snugly around the flange. Determining the true size of the O-ring that best fits the flange is very difficult because small changes in the cut length make the difference between whether it fits snugly or not. The equation for calculating the cut length of an O-ring is

$$L = \pi \left(\frac{OD + ID}{2} \right), \quad (2.1)$$

where OD stands for the outer diameter and ID for the inner diameter which is calculated using:

$$ID = OD - 2 \times (C_s), \quad (2.2)$$

where C_s is the cross sectional diameter of the cord. These equations have been extremely helpful in determining the appropriate dimensions needed to manufacture an O-ring.

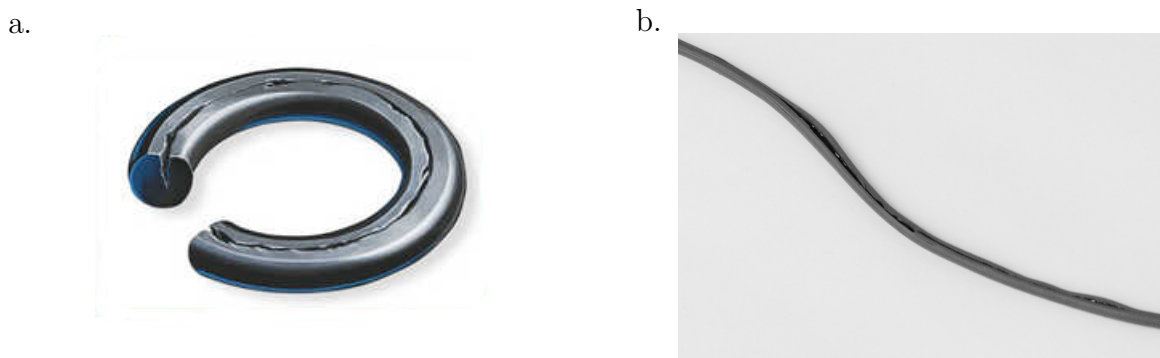


Figure 2.3: O-ring over compression failure
a. reference photo[6] b. actual O-ring

In addition to engineering an O-ring, diagnosing the failure of one is also very important. In April 2012 the initial O-ring broke due to over-compression, resulting from too much pressure and high temperatures due to baking. A stable fix to this obstacle is still in development. After several failed attempts to purchase the correctly sized O-ring from manufacturers a temporary solution was achieved with a razor blade and some cyanoacrylate adhesive (super glue). The details of how we constructed the new O-ring is in appendix D. Minimizing the over-compression and preventing the breaking of the cyanoacrylate bond of a temporary O-ring is done by monitoring baking temperatures via an infrared thermometer. Exercising caution in avoiding the temperature limits, usually 80°C , specified by the manufacturer of the cyanoacrylate will prevent other more serious problems that would ensue if the seal broke.

2.1.3 Vacuum Conditioning

Vacuum conditioning and upkeep aids in achieving consistent results from in vacuum experiments. A vacuum system left alone at atmospheric pressure will require a several days of conditioning prior to use for research, due to water vapor build-up [7]. We condition our vacuum chamber using two techniques. The first,

commonly known as baking, reduces outgassing through heating the chamber walls and components. The second technique is to backfill the chamber with a dry gas such as argon, nitrogen, etc., which has a “molecular scrubbing” effect. The procedure for conditioning the chamber is found in appendix D.

Water vapor is the most detrimental molecule in most vacuum systems. Because water molecules adsorb easily onto clean surfaces, it is difficult to remove them from vacuum systems [7]. Removing many of the monolayers of water from the stainless steel walls takes anywhere from several hours to days. Accelerating desorption of water molecules is achieved by providing additional energy via heat tape on the outside of the chamber. An RGA can characterize desorption of water monolayers during baking (see figure 2.5). Note how the partial pressure due to water vapor gradually decreases over time. If this same process was repeated without baking, desorption of water would occur more slowly. Baking via heating tape is a low cost solution for conditioning a vacuum. There are alternatives that are more effective such UV radiation and sputtering with an inert gas [7].

In addition to baking, the practice of backfilling, or refilling a vacuum with a dry gas, is another common technique used to clean systems. Argon is probably the most common gas used because of its large atomic size, which makes it better for sputtering off unwanted molecules from chamber walls. However, dry nitrogen is a more cost effective alternative that also works fairly well. Molecular “scrubbing” works by adding molecules, in this case nitrogen gas, which then collide with adsorbed molecules “knocking” them off so they will be pumped out. This is best done near the crossover pressure of the roughing pump, and requires the use of a leak valve to precisely control the backfilling of dry nitrogen. The crossover pressure is the pressure at which the pump can no longer keep up with the gas load it is under. Carrying out both conditioning processes simultaneously yields better results

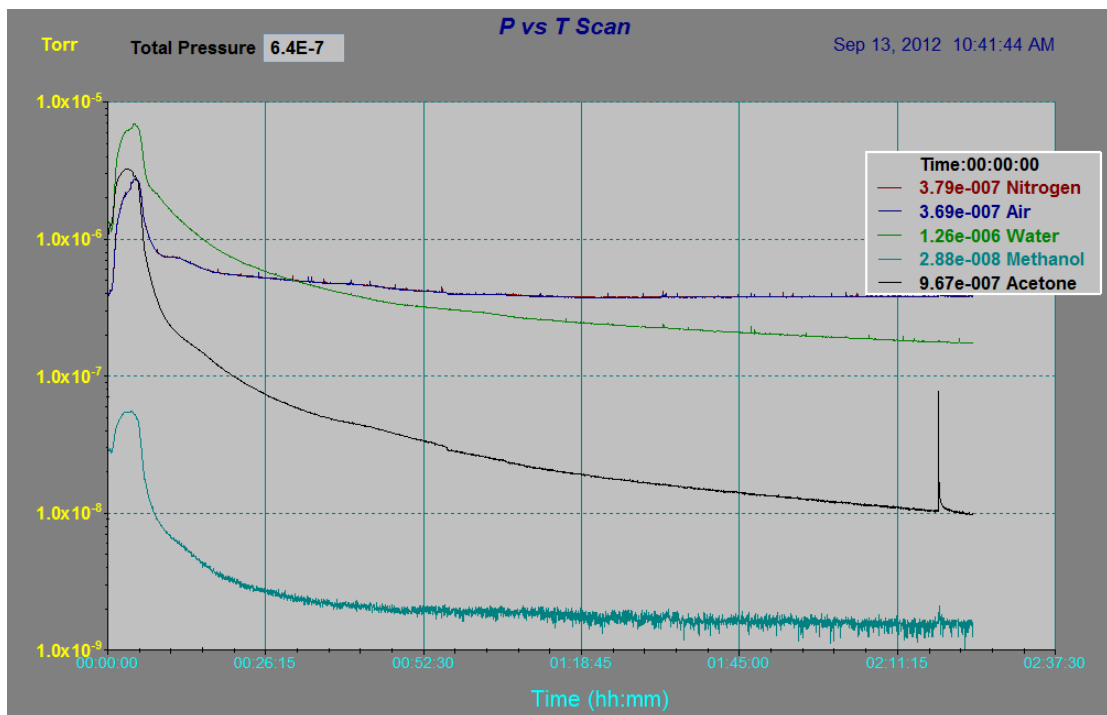


Figure 2.4: RGA P vs T graph

than they would separately. Implementing additional conditioning methods would show only minimal improvement until a better process for transferring material into and out of the chamber is developed so that the 25" flange can remain sealed. The best practice for keeping a vacuum clean is to avoid putting anything in it that would contaminate its surfaces.

2.2 Deposition System Design

2.2.1 The Original Experiment

Designing a deposition system is remarkably difficult. Knowing the difficulty, it is understandable that flashing metal wire created the first films. Essentially, flashing, or flash evaporation, occurs when you run a high current through a wire so that it sublimates. The original flashing experiment at BYU-Idaho used a nickel-silver alloy

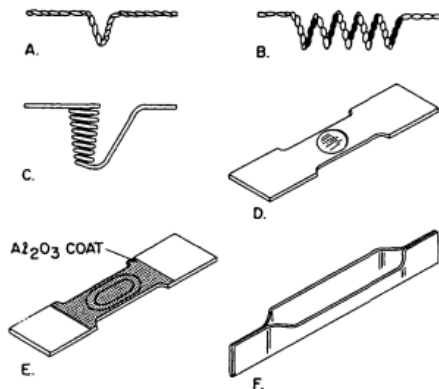


Figure 2.5: Various boats and baskets [1]

wire wrapped around a tungsten wire. Unfortunately, during the flashing the tungsten sublimated and created a nonhomogeneous film on the glass substrate instead of the nickel-silver. Research done by Phillip Scott helped improve this process by exploring the use of boats and baskets (see figures 2.5 and 2.6). In addition, gradual Joule heating became the method for heating the deposition material. With these improvements came an added ability to control the deposition process, but there were still problems with homogeneity and sustainability.

2.2.2 New Crucibles & Improved Temperature Calculations

Because of these improvements, and a need for more uniform films for another research project, we began developing films and to determine their thickness experimentally (see chapter 4). Initially things went well, but the baskets kept melting during use. We tried tungsten baskets and alumina coated tungsten baskets, as suggest by the tables in appendix A, and both kept melting (see figure 2.6). The baskets kept breaking at the same spot along the wire so we began investigating the use of a stranded tungsten basket that holds a crucible, which has proven to be hardier than the smaller baskets.

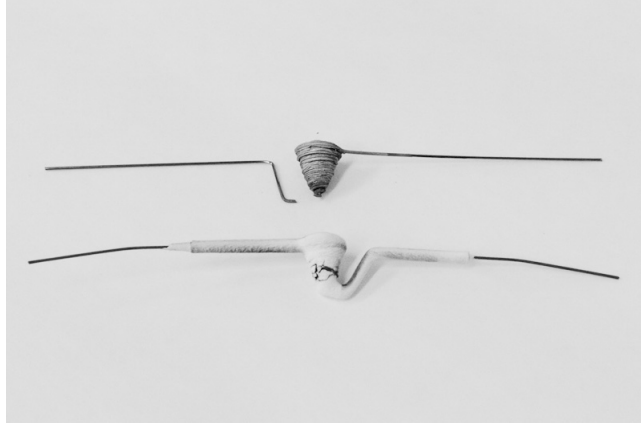


Figure 2.6: Broken tungsten baskets

An exploration of the theory behind Joule heating revealed the baskets were breaking because of the wire's small diameter. Joule proposed that the heat lost by a wire filament with a known resistance and current passing through it is proportional to $I^2 R$, where R represents the resistance. In our case, we assumed all of the power \mathcal{P} was lost in the form of heat through the filament. Thus we approximate that

$$\mathcal{P} = I^2 R. \quad (2.3)$$

Incorporating the definition of resistance, which is $R \equiv \rho \frac{l}{A_{cs}}$, where ρ is the resistivity of the material, l is the length, and A_{cs} is the cross sectional area, we end up with

$$\mathcal{P} = I^2 \rho \frac{l}{A_{cs}}. \quad (2.4)$$

Using this equation, in conjunction with values found in the CRC Handbook for the emissivity of tungsten [8] and the Stefan-Boltzman law,

$$\mathcal{P} = \sigma \epsilon A_s T^4, \quad (2.5)$$



Figure 2.7: Broken quartz crucibles

where σ is the Stefan-Boltzman constant, ϵ is the emissivity, A_s is the surface area of the black body, and T is the temperature; yields

$$T = \left[\frac{I^2 l \rho}{A_s A_{cs} \sigma \epsilon} \right]^{\frac{1}{4}}. \quad (2.6)$$

This equation can then be used to approximate the temperature of a wire with a known current running through it. This approximation serves two purposes, first it explains why the wire baskets began to melt, and second it provides a more accurate calculation of the temperature for calculating the deposition rate. Hence, we adopted a crucible and stranded tungsten basket combination. Although the tungsten wire won't melt until about 2300°C the crucibles will often break well before that temperature (see figure 2.7). For Al deposition, a boron nitride (BN) crucible works best because of its high thermal conductivity, and thermal resistance and its low thermal expansion [9]. A BN crucible can sustain temperatures up to roughly 1800°C without breaking. Vapor pressure curves, which can be found in appendix B, show that the Al will begin to evaporate prior to 1800°C in the 10^{-5} to 10^{-8} Torr range.

2.2.3 Power Supplies & Feedthroughs

Upgrading the heating element meant we also needed to find a more suitable power supply. The previous power supplies could only provide 20 and 40 amps, which was not enough to heat the new filament design to an adequate temperature. Joule heating requires large currents and/or high voltages to accelerate the electrons traveling through a conductor. Applying a high current is analogous to a large river of electrons moving through the structure and high voltages are similar to a strong accelerating force to the electrons. Energy is transferred to the lattice structure of the conductor as moving electrons "collide" with other atoms. Increasing the number of "collisions" or increasing the energy transferred per collision results in a greater macroscopic temperature change. To reach our desired temperature, we purchased a power supply with a power output of 750 watts (60 amps and 12.5 volts). During the research of power supplies, we reassessed the equipment that was being used and looked for improvements. The high voltage feedthrough we were using wasn't suited use with high current. To avoid future complications, we also purchased a high current feedthrough with solid oxygen free copper (OFE) leads to help reduce the power loss through the feedthrough pins. Additionally, work was done to design a new support system for connecting the tungsten filament to the copper leads. The new configuration can be seen in figure 2.8 and the previous design in figure 2.9.

2.2.4 Substrate Holder Design

Another feature of the new design is a substrate holder that won't chip the edges of the substrates. A substrate is the surface on which films are grown. In theory, the substrate consists of any type of material. However, the application usually determines the material that is used (i.e. silicon for semiconductors). As the float glass substrates were wedged between the threads of two screws positioned above



Figure 2.8: New crucible holder configuration

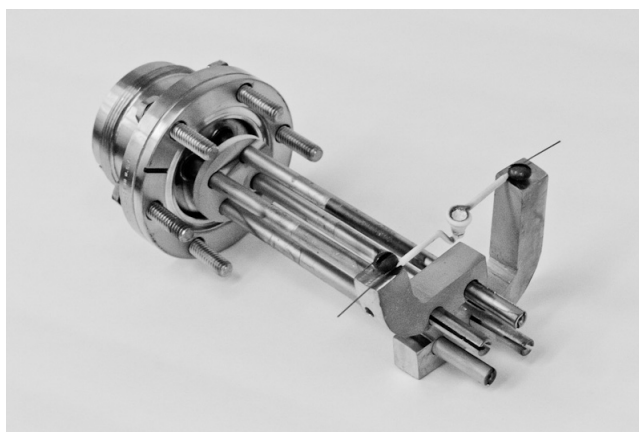


Figure 2.9: Old crucible configuration

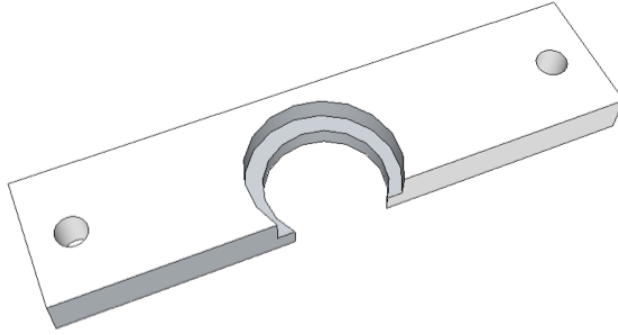


Figure 2.10: Substrate holder design

the deposition source they often chipped and damaged the slides. The remedy to this problem was to design a new holding system, seen in figure 2.10, and switch the substrate from float glass slides to round mineral watch glass. A lathe was used to craft the designed holder from Al; and it was secured in place inside the vacuum using $4\frac{1}{2}$ inch steel bolts mounted seated on a 6 inch blank flange on the top of the chamber.

The design and implementation steps for the vacuum and deposition systems represent a substantial fraction of my thesis work. However, to fully comprehend the impact these developments made on the respective systems a deeper explanation of each individual piece of equipment is given in the next chapter.

Chapter 3

Procedures & Documentation

3.1 Equipment Documentation

Purchasing equipment is an important aspect of all experimental physics research. For further information regarding part numbers or companies from which equipment was purchased, refer to appendix C. The parts purchased for this project are detailed in this section.

3.1.1 Silicon Heating Tape

The purpose of the silicon heating tape is strictly for vacuum bakeout. Capable of heating the chamber to 120°C, the heat tape is primarily designed to reduce the water vapor content of the vacuum chamber. Heating the chamber walls with the tape gives the sorbed, or adhered, water on the stainless steel the energy needed to eventually evacuate the system and thereby reducing the overall contribution to the total pressure from water vapor.

Length	72 <i>in</i>
Power density	4.3 <i>Watts/in²</i>
Note: has a high chemical resistance.	

Table 3.1: Silicon Heat Tape Specifications

Placing the heat tape flat against the chamber walls during installation provides the best thermal transfer and can prevent hot spots on the tape during use. In addition, the tape should not overlap itself at any point. The installer should be mindful of the proximity of the tape to specific chamber components to prevent damage to sensitive equipment. When installing the user should make note to only use high temperature tape to adhere the silicon to the chamber. During use, a variable transformer in conjunction with the tape will help to control the bakeout temperature of the chamber. Correct operation of the heat tape leads to lower base pressures and faster pump down times.

3.1.2 Type C Thermocouple

Thermocouples are capable of providing accurate temperature measurements both in and out of vacuum. A special feedthrough is required in order to use a thermocouple within a vacuum. There are several classifications of thermocouples that cover different temperature ranges and have varying accuracies. A type C thermocouple is used with the BYU-Idaho vacuum system, as it is capable of measuring temperatures up to 2300°C . By comparing the measured voltage across two different metals to that of a reference voltage a thermocouple can determine the temperature. For this process to determine an accurate temperature a cold junction is often required. We use this thermocouple, in conjunction with power loss calculations, to help evaluate consistency of our temperature calculations. The approximation provided by the thermocouple will assist future students in determining the melting point of the Al. Within the chamber, the hot junction is

Temperature Range	0 - 2300 °C
Positive wire	W/5% Re
Negative wire	W/26% Re
Note: Made for use in high and ultra high vacuums.	

Table 3.2: Type C thermocouple specifications

placed about an inch from the W filament so a correct temperature is read.

3.1.3 Quartz Crystal Microbalance

The quartz crystal microbalance (QCM) is one of the more costly purchases made for my research. The purpose of the QCM is to measure the deposition rate of material onto the substrate. A QCM operates on the piezoelectric principle. During use, the crystal resonates to a frequency generated by an oscillating circuit. Most cut crystals are tuned to resonate to a 6 MHz frequency, but as mass is added to the crystal during the deposition process the frequency of oscillation increases, as explained by the Saurbrey equation:[10]

$$\Delta f = -\frac{2f_0^2}{A\sqrt{\rho_q\mu_q}}\Delta m, \quad (3.1)$$

where Δf is the change in frequency, δm the change in mass, A the crystal area, f_0 the resonant frequency, $\rho_q = 2.648 \frac{g}{cm^3}$ the density of quartz, $\mu_q = 2.947 \times 10^{11} \frac{g}{cm \cdot s^2}$ the shear modulus of quartz for the crystal. Positioning the sensor head on the same spherical wave front as the substrate enables the QCM to provide a reasonable approximation for the rate of deposition. To correctly position the sensor head, the water cooling lines that support the sensor were bent, using a tube bending tool, to an angle slightly past $90^\circ C$ (see figure 3.1). In this position, the QCM software can be calibrated to provide real time graphs of the rate of deposition and film thickness. As of the moment, the QCM still needs calibration before it will provide accurate results. The calibration of the QCM is a project that future students might be

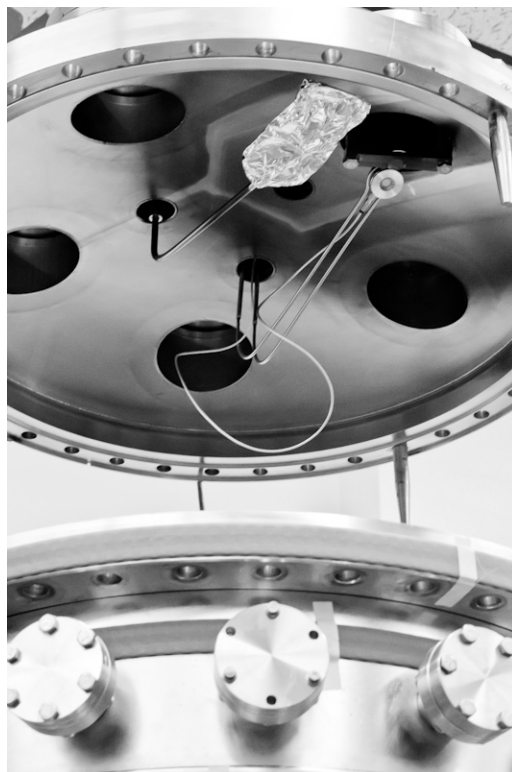


Figure 3.1: Quartz Crystal Microbalance Positioning

interested in completing. Calibration should be completed prior to collecting data.

3.1.4 Residual Gas Analyzer

The purpose of a residual gas analyzer (RGA) is to analyze the gas composition within the vacuum chamber. A quick review of how to use the RGA will help prolong its life, as all of the repairs for this piece of equipment are costly. The RGA should not be operated if the base pressure of the chamber reads a pressure higher than 10^{-5} Torr. Exposing the hot filament to the atmosphere oxidizes and ruins the filament. Second, the RGA repeller cage, which looks like a miniature Faraday cage covering the filament, tends to short with the chamber walls. When the repeller cage shorts with the chamber the software reads noise around 10^{-9} Torr. Carefully bending the repeller cage may fix the problem. If this doesn't work, you can check the resistance across the supply and return pins to test if the filament itself is bad.

For additional resources and details regarding troubleshooting, see appendix C.

3.1.5 Crucibles, Baskets, & Boats

Thermal deposition is achievable via a number of tools. Boats, baskets, wires, etc. provide different ways to heat the deposition material. The table in appendix A describes the best tools to use for heating different materials. As previously discussed, the first baskets frequently broke during use. So we switched to a stranded tungsten basked setup. Using a wire basket and crucible combination facilitates an easy transition to making films with other materials. To avoid cross contamination, each element should have its own crucible. Knowing the temperature limits of the crucible material will help to prevent breaking or damaging the crucible due to thermal stress. Appendix C also provides useful information regarding the properties of the common materials used for crucibles. Lastly, figure 3.2 contains an illustration of the current W basket.

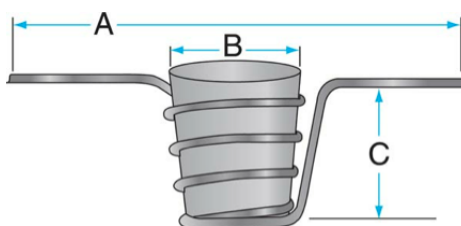


Figure 3.2: Crucible & basket combination

3.1.6 Power Supplies

Each power supply that we have used has its own pros and cons. We have used, or just recently purchased; 20, 40, and 60 amp power supplies. The most capable power supply is definitely the 60-amp supply both in features and power output. As with any piece of complex equipment, it would be wise to study the user manual prior to use. Also, when using any power supply make sure to use the proper gauge

Power Output	750 Watts
Max Current	60 Amps
Max Voltage	12.5 Volts
Features: OVP, UVP, Foldback & over-temperature protection	

Table 3.3: Genesys 60-12.5 power supply details

for the load cables for the intended power transmission. Connecting several load cables in parallel works in a pinch to prevent the wires from overheating.

Over voltage protection (OVP) and under voltage protection (UVP) are features of the Genesys 60-12.5 power supply that allow the user to set a maximum or minimum output voltage respectively. Foldback protection is an overload protection feature that lowers the output voltage and current to below normal levels in the event of a short circuit.

3.2 Vacuum Procedures

As a forewarning, neglecting to follow the outlined procedure for use of the vacuum chamber may damage pumps, gauges, or the chamber itself. In almost all cases, it is beneficial to leave the chamber in a low vacuum state. There is no limit to how long the chamber may remain at low vacuum as the lower pressure helps prevent the sorbtion of water onto the stainless steel walls. Leaving the oil diffusion pump on at all times is impractical as the oil takes approximately two hours to cool and may crack if the power went out.

3.2.1 Pumping to Low Vacuum

1. Turn on the pressure gauge controller and verify that the chamber is pressurized.

2. Close all vent or leak valves that connect the chamber or pumps to the atmosphere. For the large flange make sure that the Viton O-ring fits snugly in its groove before closing the chamber lid.
3. Open the gate valve between the chamber and diffusion pump, and the ball valve connecting the roughing pump to the diffusion pump.
4. Turn on the roughing pump.
5. Wait until the pressure controller for the chamber reads $\sim 10^{-3}$ Torr.

3.2.2 Pumping to High Vacuum

1. Make sure that the thermocouple gauge for the chamber reads $\sim 8 \times 10^{-3}$ Torr.
2. Turn on the water cooling for the diffusion pump.
3. Plug in the diffusion pump, and wait until the heating element reaches 170°C .
4. Wait another five minutes for the diffusion pump to reach approximately 10^{-5} Torr.
5. Turn on the ion gauge and RGA as necessary.

Procedure for Removing Slides

1. After turning off the power supply and giving the crucible time to cool proceed with the following steps.
2. If the ion gauge or RGA are on, turn them off.
3. Firmly close the gate valve between the chamber and diffusion pump.
4. Confirm that the valve between the chamber and the roughing pump is also closed.
5. Vent the chamber.
6. Open the chamber, retrieve/replace the slide, place the Viton O-ring on the flange, and shut the chamber.
7. Close the vent valve to the chamber.
8. Close the ball valve between the diffusion and roughing pumps. This step should be done as quick as possible to prevent the diffusion pump from pressurizing, which can result in cracked oil.
9. Open the valve between the chamber and the roughing pump.
10. Pump down to $\sim 10^{-3}$ Torr.

11. Open the gate valve and the ball valve.
12. Close the valve between the chamber and roughing pump.
13. Turn on any gauges as necessary.

3.3 Deposition Procedure

The deposition process is still under development. Some factors, such as slide outgassing, have been investigated but the effects aren't fully known. It is best to clean the slides with methanol or isopropyl alcohol and then let cleaning agent evaporate fully prior to placement in the chamber. Recording more data will help future students to better tune this process and improve control over film characteristics.

1. Weigh the glass slide after cleaning and prior to placing it in the chamber.
2. While the chamber is open place a few Al pellets in the BN crucible.
3. Also, position the shield at 55° to cover the substrate.
4. After reaching a high vacuum connect the power supply to the feedthrough.
5. Turn on the power supply and turn the voltage control all the way up so the power output is dependent on the current control knob.
6. Slowly increase the current output. This is done by increasing the output by 3-5 amps and then waiting a few minutes for the crucible to reach a thermal equilibrium with the W basket.
7. At the desired power output & temperature turn the mechanical feedthrough clockwise to move the shield out of the way.
8. During deposition record the time elapsed, power supply settings, and the chamber pressure before and during the deposition process.
9. When done, decrease the current output in the same manner that you increased it (you can decrement the current in larger amounts) and eventually turn off the power supply.
10. Lastly, immediately after opening the chamber measure mass of the slide.

Chapter 4

Thin Film Deposition Rates

4.1 Initial Rate Calculations

A simple method for approximating the rate of deposition during deposition is done by weighing the slides pre- and post-deposition and then calculating the average rate by using equation 4.1. This method is difficult and is prone to many additional factors that don't affect rates calculated by equipment such as a QCM. The purchase of the QCM actually came after this experiment failed to determine a realistic rate. The rate calculated by the Langmuire-Knudsen equation gives the rate in units of grams per square centimeter seconds. The experimental rate should look like

$$R_{exp} = \frac{m}{At}. \quad (4.1)$$

The mass m in the equation is the change in mass, or the mass of Al deposited, of the slide. Measuring the slide pre and post deposition is an easy task, but the scale used needs to be capable of measuring differences of milligrams at minimum.

Calculating the filmed area of the slide required a more creative approach. After projecting a filmed slide onto a wall and tracing the filmed area onto grid paper, we were able to approximate the deposition area via a scale and the number of filmed squares on the grid paper. Figure 4.1 shows a copy of the grid paper where the

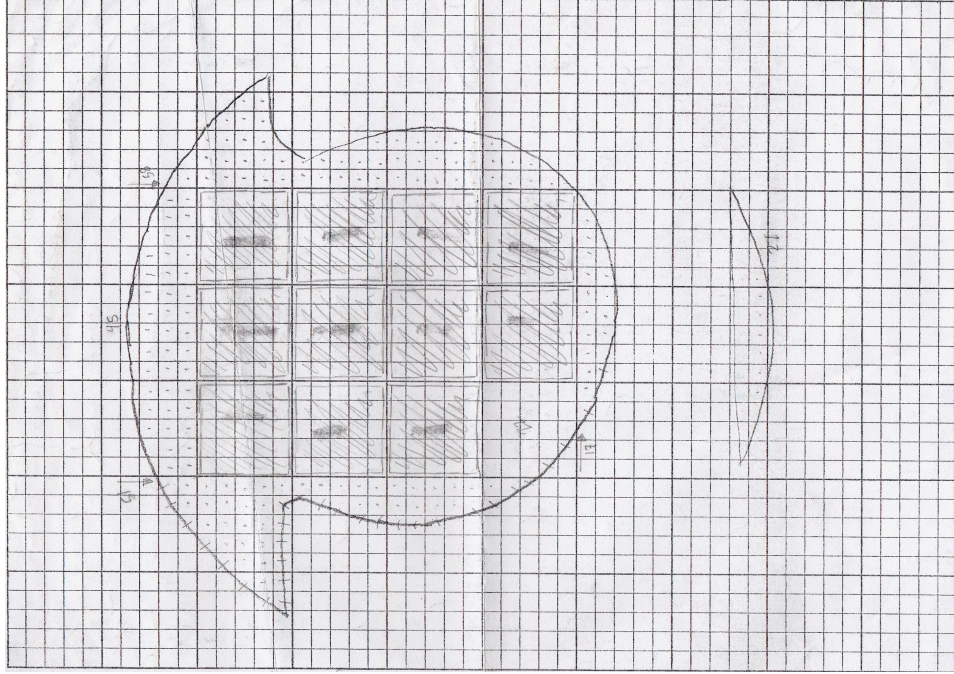


Figure 4.1: Filmed slide projection

shaded squares represent the filmed area.

Assuming no angular dependence in the Langmuire-Knudsen equation further simplifies the theoretical model to look like

$$R_m = C_m \sqrt{\frac{M}{T}} \frac{1}{r^2} (P_e(T) - P). \quad (4.2)$$

This justification is acceptable given the crucible is positioned directly beneath and sufficiently far from the substrate[11]. An appropriate distance should meet the requirement that the mean free path of molecules in the chamber be much greater than the distance between the crucible and substrate. Black body temperature approximations include an emissivity factor relating to the fraction of power that is emitted as radiation. For initial calculations we used an emissivity of one. Realistically the emissivity of tungsten between 1700 and $2500^\circ C$ is roughly 0.41 [8]. Using an accurate emissivity doesn't change the outcome of the early experiment.

The uncertainty in the temperature calculations was the biggest factor affecting the deposition rate calculations. Initial temperature calculations had an uncertainty of $\pm 75^{\circ}\text{C}$. Improving the accuracy of temperature calculations may make this method reasonable.

Calculating the uncertainties associated with the composition of equations is a mathematical mess. MATLAB code for analyzing the data and determining the χ^2_{ν} value is in appendix F. This code accounts for the effects of slide outgassing while in vacuum by adding an empirically calculated amount as well as a coefficient for the black body emissivity and its related uncertainty.

The data from the experiment indicates that our model is far from accurate. Data from eleven slides was analyzed to compare the theoretical deposition rate under the given conditions and deposition time to the experimentally calculated rate. The reduced χ^2 value was around 3.3×10^7 . This alludes to the inadequacy of the tested model in calculating the deposition rate of Al vapor. Despite the results the experiment was useful in determining several areas of improvement for the deposition system and the process used for calculating rates.

4.2 Effects of Slide Outgassing

After measuring a post-deposition slide mass that was less than its pre-deposition weight, we realized that the mineral glass must have been outgassing. So we devised an experiment to quantify the slide outgassing. Determining how much a material outgasses is simple. After cleaning each slide individually and letting the methanol evaporate off, they were weighed and placed inside the vacuum chamber. To maintain a controlled environment all of the slides were placed side-by-side inside

the vacuum for the same length of time. After several hours the slides were removed and weighed. Weighing each slide daily for several days after the experiment provided additional insight about the environmental effects on the slide's weight. Figures 4.2 and 4.3 show the change in each slides weight over the course of several days.

The average change in slide mass between pre and post outgassing was 0.0012 grams. This is the same value used to adjust for the weight lost during the film deposition process. Adjusting the weight due to outgassing effects improves the accuracy of calculated rates. Producing thicker films in the future would negate most of the effects from outgassing as the difference in slide mass would be more significant with a thicker layer of Al deposited on them. Further inquiry into the causes that influence the weight of a slide on a given day would be helpful as well. The data suggests that environmental factors such as humidity and room temperature may play a more crucial role in the weight of a slide than was at first believed.

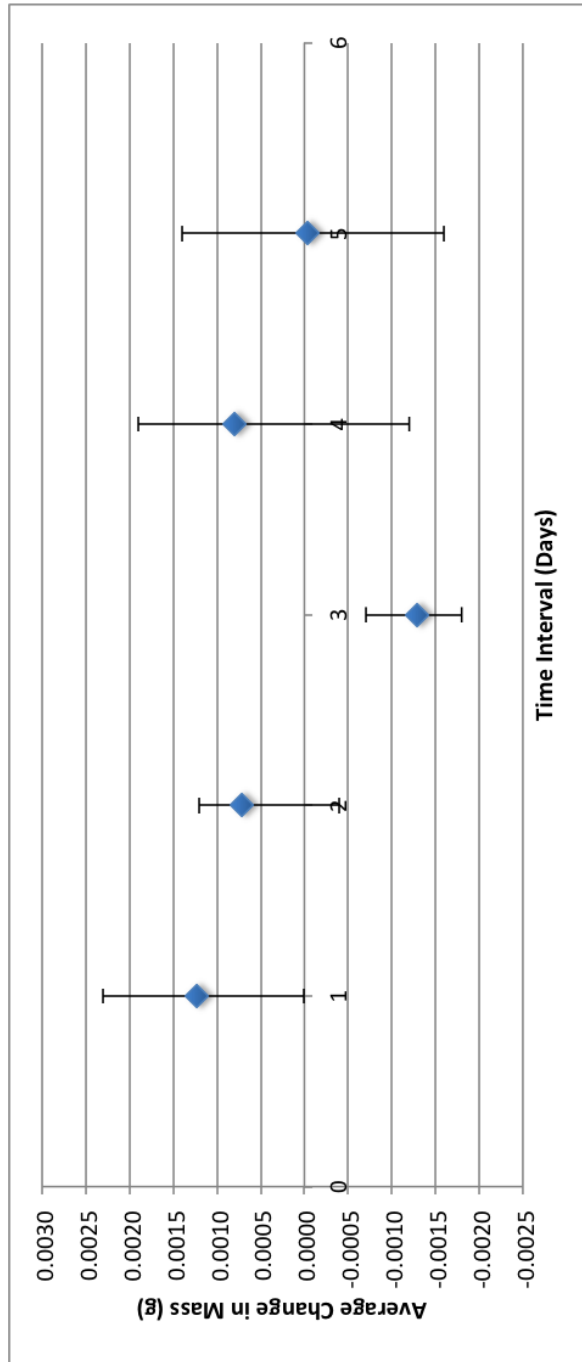


Figure 4.2: Average change in slide mass over time

The initial time interval is the difference between the initial and post outgassing weights. The error bars also provide the high and low deviation from the mean change in mass.

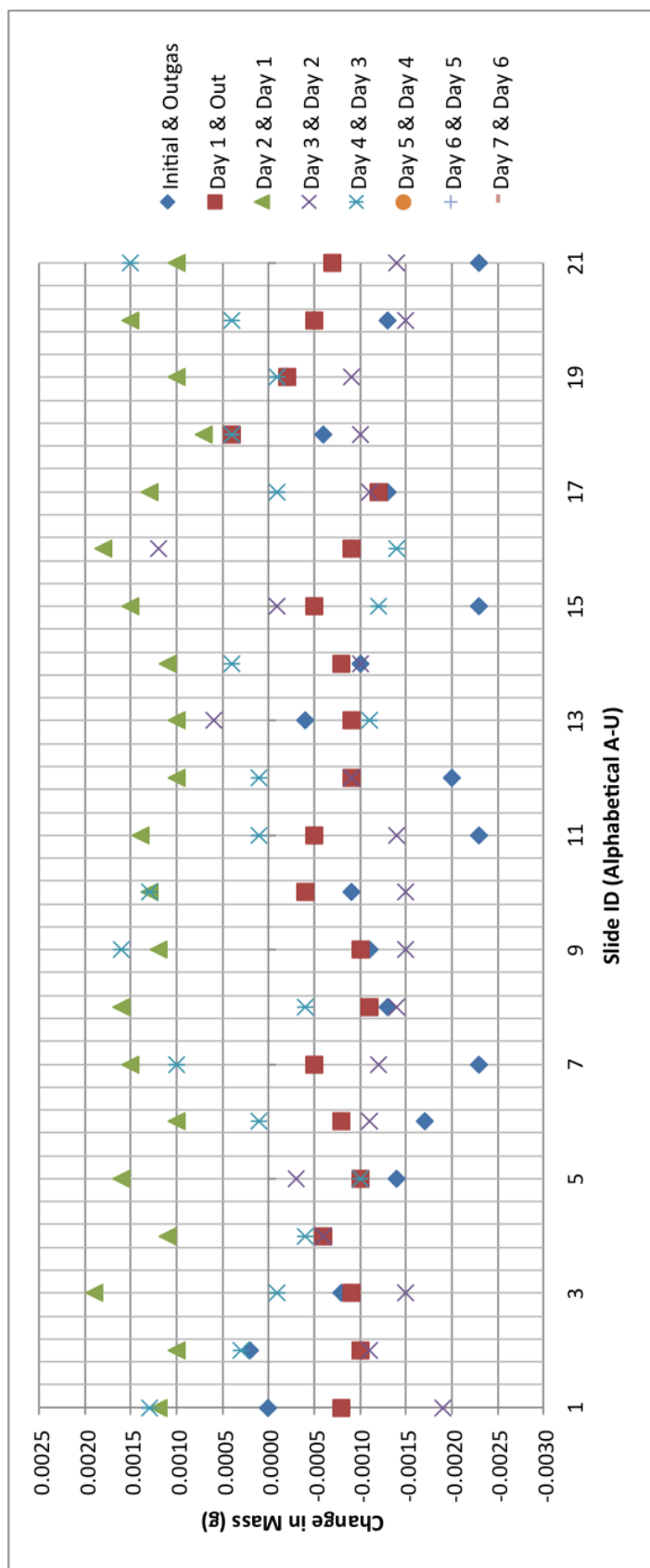


Figure 4.3: Change in slide mass between consecutive days

Chapter 5

Future Experiments & Summary

Fully automating the deposition system is still a long ways down the road. This means there is an ample supply of projects left for future students. Developing the system will expand the research opportunities for future students enabling them to conduct experiments requiring the use of films. Since we are now able to consistently produce films, students may want to work on improving film quality and deposition rate calculations. In addition, it may interest some students to look into alternative deposition methods.

5.1 Improving Film Quality

There are two sides to improving film quality. The first is the ability to recognize and characterize a films quality. This is known as film tribology. The other side emphasizes applying methods for ensuring the desired film characteristics during deposition. Film tribology requires additional equipment that we currently don't own. Using this equipment characteristics of films such as adhesion, hardness, and homogeneity can be determined. Some of the tribology methods are also an effective

at determining film thickness after deposition. Students wanting to learn more about film tribology would find the *Handbook of Hard Coatings* helpful in their research[12]. This book also contains ample information regarding many CVD and PVD methods and their theory.

An important step in building a quality deposition system is implementing preventative methods. Better substrate preparation is one item requiring more attention, and something that would definitely improve the film quality. Typical substrate preparation often involves chemical etching and cleaning prior to deposition followed by heating during and after deposition to anneal the film and/or bias the substrate surface. These methods would also require new equipment. Methods such as e-beam or sputter deposition can also provide improved film quality and purity. Ample resources regarding the best practices regarding film quality are available in many of the cited texts.

5.2 Improved Deposition Rates

During the rates experiment we made several questionable approximations to calculate our theoretical rates. A few alternative approximations still exist that may improve results. This may lead to practical application in calibrating the QCM and use with films of other materials. Analyzing the magnitude of uncertainties of variables in an experiment can be quite revealing of what needs improvement. Such is the case with the deposition rates, and the variable with the largest uncertainty is the temperature. We believe the large uncertainty in the temperature to be related to the significant amount of power that is lost by the load cables. Preliminary calculations suggest that the actual voltage across the W basket used to heat the crucible is significantly less than previously believed. Incorporating the loss of

power during transmission may improve the accuracy and precision of the calculated temperature.

These projects are just a few of many that would be valuable for future students wanting to work with the BYU-Idaho vacuum and deposition systems. Excellent opportunities for research still exist for students. Unlike the deposition system, the vacuum system has limited room for further development without conducting a complete overhaul. However, this doesn't limit the possibilities for research in any way.

Bibliography

- [1] John L. Vossen and Werner Kern. *Thin Film Processes II*. Boston: Academic Press, 1991.
- [2] James M. Lafferty. Vacuum: from art to exact science. *Physics Today*, 34(11):211–231, 1981.
- [3] D.M. Mattox. *Foundations of Vacuum Coating Technology*. William Andrew Publishing/Noyes, 2003.
- [4] John F. O’Hanlon. *A User’s Guide to Vacuum Technology*. John Wiley ‘&’ Sons, Inc., 3rd edition, 2003.
- [5] Wake Forest University. Vacuum evaporation. PDF, Mar. 2012. URL: http://users.wfu.edu/ucerkb/Nan242/L06-Vacuum_Evaporation.pdf.
- [6] Problem Solving Problems Inc. O-ring and seal failure [online]. URL: <http://www.pspglobal.com/abrasion.html>.
- [7] D.M. Mattox. *Handbook of Physical Vapor Deposition (PVD) Processing*. William Andrew Publishing/Noyes, 1st edition, 1998.
- [8] Robert C. Weast, editor. *Handbook of Chemistry and Physics*. CRC Press, Inc., 66th edition, 1985.
- [9] Accuratus. Ceramic materials’ character [online]. URL: <http://accuratus.com/materials.html>.

- [10] Stanford Research Systems. Quartz crystal microbalance theory and calibration. PDF. URL: <http://www.thinksrs.com/downloads/PDFs/ApplicationNotes/QCMTheoryapp.pdf>.
- [11] M. A. Herman, H. Sitter, and W. Richter. *Epitaxy: Physical Principles and Technical Implementation*. Springer-Verlag, 2010.
- [12] R. F. Bunshah. *Handbook of Hard Coatings*. Norwich, N.Y.: Noyes Publications and Park Ridge, N.J.: William Andrew Pub., 2001.
- [13] Jonathan Stolk. Materials guide for thermal evaporation [online]. Jan. 2012. URL: http://www.lesker.com/newweb/menu_depositionmaterials.cfm?section=MDtable.
- [14] Dr. Walter Umrath. Fundamentals of vacuum technology. Technical report, Oerlikon Leybold Vacuum, 2007.

Appendix A

Materials Guide for Thermal Evaporation

Adapted from Kurt J.Lesker Co. [13]

Key of Symbols

*influenced by composition ** Cr-plated rod or strip ***All metals alumina coated Ex = excellent G = good F = fair P = poor S = sublimes D = decomposes C = carbon Gr = graphite
Q = quartz Incl = Inconel VC = vitreous carbon SS = stainless steel

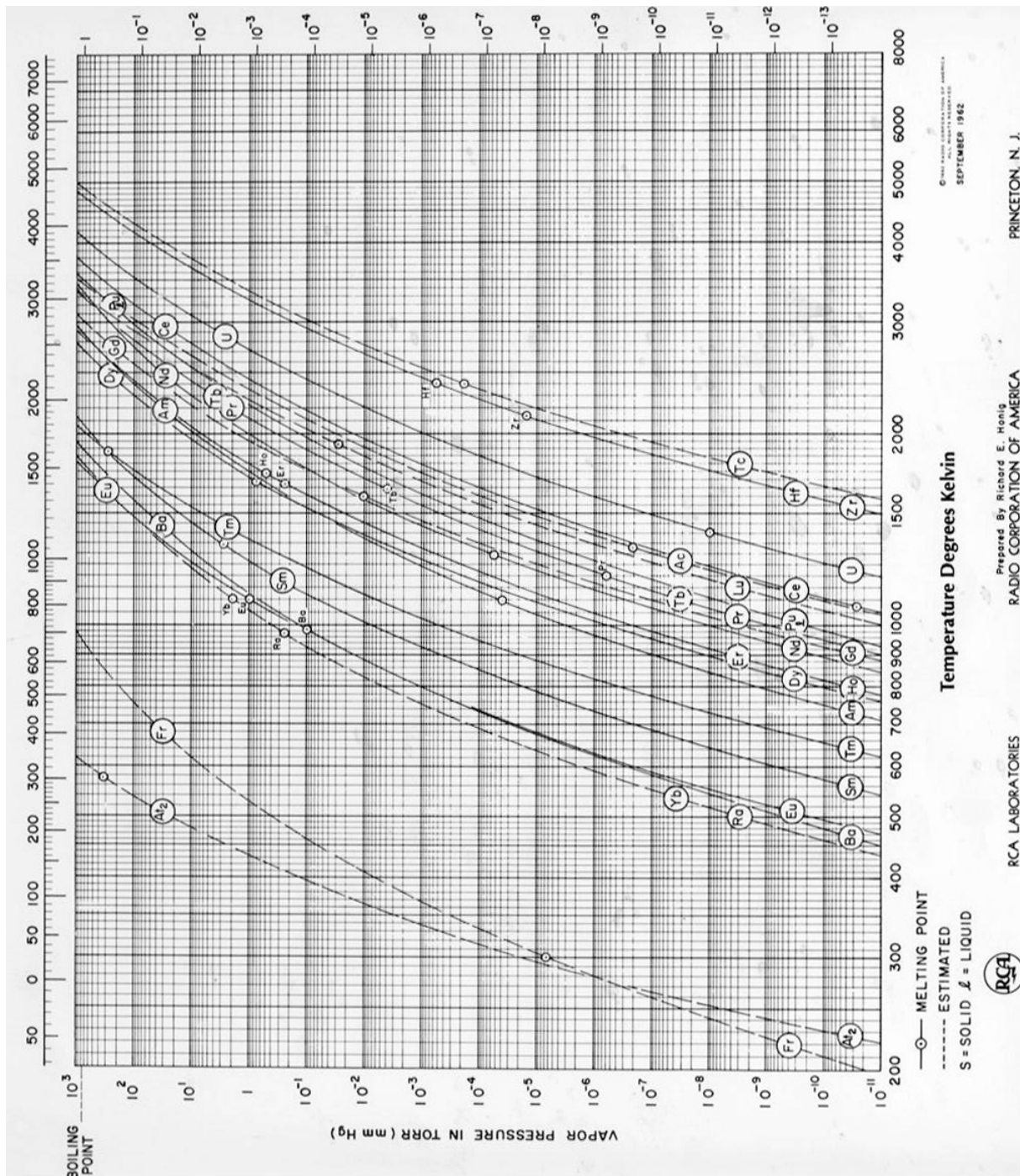
Material	Formula / Symbol	MP (°C)	Sublime / Decompose	ρ (g/cm ³)	Temp. (°C) for Given Vap. Press. (Torr)			Thermal Sources			Comments
					10-8	10-6	10-4	Boat	Coil	Basket	
Aluminum	Al	660		2.70	677	821	1010	TiB ₂ W	W	W	Alloys and wets. Stranded W is best.
Aluminum Antimonide	AlSb	1080		4.30	-	-	-	-	-	-	-
Aluminum, 2% Copper	Al2%Cu	640		2.82	-	-	-	-	-	-	Wire feed and flash. Difficult from dual sources.
Aluminum, 2% Silicon	Al2%Si	640		2.69	-	-	1010	-	-	-	Wire feed and flash. Difficult from dual sources.
Antimony	Sb	630	S	6.68	279	345	425	Mo,*** Ta***	Mo, Ta	Mo, Ta	Toxic. Evaporates well.
Barium	Ba	725		3.51	545	627	735	W, Ta, Mo	W	W	Wets without alloying reacts with ceramics.
Beryllium	Be	1278		1.85	710	878	1000	W, Ta	W	W	Wets W/Mo/Ta. Powder and oxides toxic. Evaporates easily.
Bismuth	Bi	271		9.80	330	410	520	W, Mo, Ta	W	W	Toxic vapor. Resistivity high. No shorting of baskets.
Boron	B	2300		2.34	1278	1548	1797	C	-	-	Explodes with rapid cooling. Forms carbide with container.
Cadmium	Cd	321		8.64	64	120	180	W, Mo, Ta	-	W, Mo, Ta	Bad for vacuum systems. Low sticking coefficient.
Cadmium Antimonide	Cd ₃ Sb ₂	456		6.92	-	-	-	-	-	-	-
Calcium	Ca	839	S	1.54	272	357	459	W	W	W	Corrodes in air.
Carbon	C	~3652	S	1.8-2.1	1657	1867	2137	-	-	-	E-beam preferred. Arc evaporation. Poor film adhesion.
Cerium	Ce	798		~6.70	970	1150	1380	W, Ta	W	W, Ta	-
Cesium	Cs	28		1.88	-16	22	80	SS	-	-	-
Chiolote	NasAlF ₁₄	-		2.90	-	-	~800	Mo, W	-	-	n = 1.33
Chromium	Cr	1857	S	7.20	837	977	1157	**	W	W	Films very adherent. High rates possible.
Cobalt	Co	1495		8.90	850	990	1200	W, Nb	-	W	Alloys with refractory metals.
Copper	Cu	1083		8.92	727	857	1017	Mo	W	W	Adhesion poor. Use interlayer (Cr). Evaporates using any source material.
Dysprosium	Dy	1412		8.55	625	750	900	Ta	-	-	-
Erbium	Er	1529	S	9.07	650	775	930	W, Ta	-	-	-

Europlum	Eu	822	S	5.24	280	360	480	W, Ta	-	-	Low tantalum solubility.
Gadolinium	Gd	1313		7.90	760	900	1175	Ta	-	-	High tantalum solubility.
Gallium	Ga	30		5.90	619	742	907	-	-	-	Alloys with refractory metals. Use E-beam gun.
Germanium	Ge	937		5.35	812	957	1167	W, C, Ta	-	-	Excellent films from E-beam guns.
Gold	Au	1064		19.32	807	947	1132	W	W	W*** Mo***	DC, RF, Films soft, not very adherent.
Hafnium	Hf	2227		13.31	2160	2250	3090	-	-	-	-
Holmium	Ho	1474		8.80	650	770	950	W, Ta	W	W	-
Inconel	Ni/Cr/Fe	1425		8.50	-	-	-	W	W	W	Use fine wire wrapped on tungsten. Low rate required for smooth films.
Indium	In	157		7.30	487	597	742	W, Mo	-	W	Wets tungsten and copper. Use molybdenum liner.
Iridium	Ir	2410		22.42	1850	2080	2380	-	-	-	-
Iron	Fe	1535		7.86	858	998	1180	W	W	W	Attacks tungsten. Films hard, smooth. Preheat gently to outgas.
Kanthal	FeCrAl	-		7.10	-	-	-	W	W	W	-
Lanthanum	La	921		6.15	990	1212	1388	W, Ta	-	-	Films will burn in air if scraped.
Lead	Pb	328		11.34	342	427	497	W, Mo	W	W, Ta	Toxic.
Lithium	Li	181		0.53	227	307	407	Ta, SS	-	-	Metal reacts quickly in air.
Lutetium	Lu	1663		9.84	-	-	1300	Ta	-	-	-
Magnesium	Mg	649	S	1.74	185	247	327	W, Mo, Ta, Cb	W	W	Extremely high rates possible.
Manganese	Mn	1244	S	7.20	507	572	647	W, Ta, Mo	W	W	-
Mercury	Hg	-39		13.55	-68	-42	-6	-	-	-	-
Molybdenum	Mo	2610		10.20	1592	1822	2117	-	-	-	Films smooth, hard. Careful degas required.
Neodymium	Nd	1021		7.01	731	871	1062	Ta	-	-	Low tantalum solubility.
Nichrome IV	Ni/Cr	1395		8.50	847	987	1217	***	W	W, Ta	Alloys with refractory metals.
Nickel	Ni	1455		8.90	927	1072	1262	W	W	W	Alloys with refractory metals. Forms smooth adherent films.
Niobium	Nb	2468		8.57	1728	1977	2287	W	-	-	Attacks tungsten source. n = 1.80
Niobium-Tin	Nb ₃ Sn	-		-	-	-	-	-	-	-	Co-evaporate from two sources.
Osmium	Os	2700		22.48	2170	2430	2760	-	-	-	-
Palladium	Pd	1554	S	12.02	842	992	1192	W	W	W	Alloys with refractory metals. Rapid evaporation suggested.
Parylene	C ₆ H ₈	300-400		1.10	-	-	-	-	-	-	Vapor-depositable plastic.
Permalloy	Ni/Fe	1395		8.70	947	1047	1307	W	-	-	F, Film low in nickel.
Phosphorus	P	44.1		1.82	327	361	402	-	-	-	Material reacts violently in air. n = 2.14
Platinum	Pt	1772		21.45	1292	1492	1747	W	W	W	Alloys with metals. Films soft, poor adhesion.
Plutonium	Pu	641		19.84	-	-	-	W	-	-	Toxic, radioactive.
Polonium	Po	254		9.40	117	170	244	-	-	-	Radioactive.
Potassium	K	63		0.86	23	60	125	Mo	-	-	Metal reacts rapidly in air. Preheat gently to outgas.
Praseodymium	Pr	931		6.77	800	950	1150	Ta	-	-	-
Rhenium	Re	3180		20.53	1928	2207	2571	-	-	-	Fine wire will self-evaporate.
Rhodium	Rh	1966		12.40	1277	1472	1707	W	W	W	E-beam gun preferred.
Rubidium	Rb	39		1.48	-3	37	111	-	-	-	-
Ruthenium	Ru	2310		12.30	1780	1990	2260	W	-	-	-
Samarium	Sm	1074		7.52	373	460	573	Ta	-	-	-
Scandium	Sc	1541		2.99	714	837	1002	W	-	-	Alloys with tantalum.
Silicon	Si	1410		2.32	992	1147	1337	W, Ta	-	-	Alloys with tungsten; use heavy tungsten boat. SiO produced above 4 x 10 ⁻⁶ Torr. E-beam best.
Silver	Ag	962		10.50	847	958	1105	W	Mo	Ta, Mo	DC, RF
Sodium	Na	98		0.97	74	124	192	Ta, SS	-	-	Preheat gently to outgas. Metal reacts quickly in air. n = 4.22
Strontium	Sr	769		2.60	239	309	403	W, Ta, Mo	W	W	Wets but does not alloy with refractory metals. May react in air.
Supermalloy	Ni/Fe/Mo	1410		8.90	-	-	-	-	-	-	Sputtering preferred; or co-evaporate from two sources, permalloy and molybdenum.
Tantalum	Ta	2996		16.60	1960	2240	2590	-	-	-	Forms good films.
Technetium	Tc	2200		11.50	1570	1800	2090	-	-	-	-
Teflon	PTFE	330		2.90	-	-	-	W	-	-	Baffled source. Film structure doubtful.
Tellurium	Te	452		6.25	157	207	277	W, Ta	W	W, Ta	Toxic. Wets without alloying. n = 1.002
Terbium	Tb	1356		8.23	800	950	1150	Ta	-	-	-
Thallium	Tl	304		11.85	280	360	470	W, Ta	-	W	Very toxic. Wets freely.
Thorium	Th	1875		11.70	1430	1660	1925	W, Ta, Mo	W	W	Toxic, radioactive.
Thulium	Tm	1545	S	9.32	461	554	680	Ta	-	-	-
Tin	Sn	232		7.28	682	807	997	Mo	W	W	Wets molybdenum. Use tantalum liner in E-beam guns.
Titanium	Ti	1660		4.50	1067	1235	1453	W	-	-	Alloys with refractory metals; evolves gas on first heating.
Tungsten	W	3410		19.35	2117	2407	2757	-	-	-	Forms volatile oxides. Films hard and adherent.
Uranium	U	1132		19.05	1132	1327	1582	Mo, W	W	W	Films oxidize.
Vanadium	V	1890		5.96	1162	1332	1547	W, Mo	-	-	Wets molybdenum. E-beam-evaporated films preferred. n = 3.03
Ytterbium	Yb	819	S	6.96	520	590	690	Ta	-	-	-
Yttrium	Y	1522		4.47	830	973	1157	W, Ta	W	W	High tantalum solubility.
Zinc	Zn	420		7.14	127	177	250	Mo, W, Ta	W	W	Evaporates well under wide range of conditions.
Zinc Antimonide	Zn ₃ Sb ₂	570		6.33	-	-	-	-	-	-	-
Zirconium	Zr	1852		6.49	1477	1702	1987	W	-	-	Alloys with tungsten. <F>Films oxidize readily.
Zirconium Silicide	ZrSi ₂	1700		4.88	-	-	-	-	-	-	-

Vapor pressure curves







Appendix C

Equipment Purchasing Information

Type C Thermocouple

Purchased from Kurt J. Lesker, which can be found online at www.lesker.com.

Description	Part No.	Cost
Type C CF Feedthrough	TFT3CY00003	\$295.00
Alloy 405/426 Wire*	FTAWC056	\$10.00
Note(s): *This is the type C thermocouple wire.		

Quartz Crystal Microbalance (QCM)

Purchased from Sycon Instruments, which can be found online at www.sycon.com. The QCM was purchased as a package with the STM2 and the out of vacuum BNC cable. The in vacuum microdot cable was purchased separately. All parts can be purchased directly from the company.

Description	Part No.	Cost
6 Mhz Gold Coated Sensor Crystals 10pk	500-117	\$67.00
Vacuum Feedthrough	500-017	\$491.00
Single Head Sensor	500-042	\$375.00
Oscillator & Transducer (STM-2)	500-408	\$620.00
30" Microdot Cable	500-024	\$80.00
10" Vacuum Microdot Cable	500-023	N/A

Notes: The microdot cable shouldn't be further than 30" from the sensor head while using the STM-2. Despite this we've tried to see if the STM-2 will still work with our 30" microdot cable. Preliminary findings have yielded no significant results because the power supply couldn't heat the material to a temperature that a substantial deposition rate could be detected. Additionally, the water cooling for the sensor head should be used in the future to reduce noise and improve accuracy.

Power Supplies

Several power supplies were used for thin film deposition at BYU-Idaho, but the only one purchased during my research was from TDK. The website url that the technical details can be found at is

[http : //www.us.tdk - lambda.com/hp/product_ntml/genh.htm](http://www.us.tdk-lambda.com/hp/product.html/genh.htm).

Description	Part No.	Cost
12.5V 60A Power Supply	GENH 12.5-60	\$1890.00
Note(s): We purchased the additional USB option		

Viton O-ring

Viton is used because of its low permeation rate at low pressures, and because it is resistant to many chemicals. Viton-A is the standard material used for vacuum system seals. A quick google search should provide several companies that are willing to sell Viton-A cord stock, which you can use to make your own O-rings. We are still working with a company called Quick Cut Gasket to make us some custom O-rings, but this process is time consuming and we haven't found a good fit yet. When purchasing Viton cord stock make sure you buy stock that has a cross section (CS) 0.108 inches.

Heating Tape

Purchased from BriskHeat at www.briskheat.com.

Description	Part No.	Cost
1" x 96" Silicone Heat Tape	BS0101080L	\$173.65
High Temperature Tape	PSAT36A	\$16.00

Notes: The high temperature adhesive tape is made to function up to 80°C , but we've used it past this temperature and it has held the tape in place at around 125°C .

Mineral Glass Slides

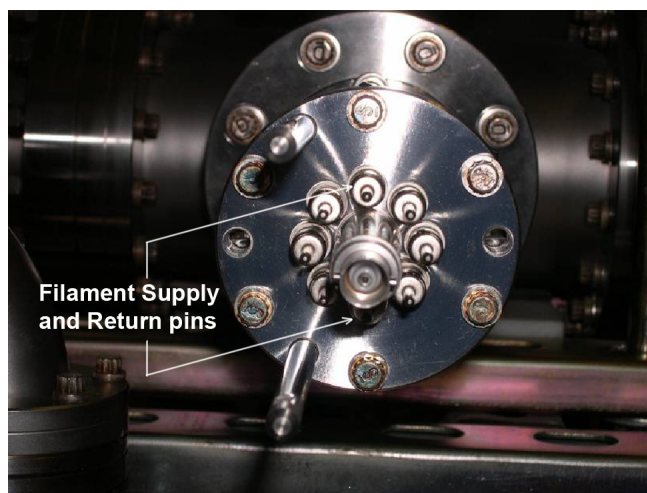
Several companies sell mineral glass slides, but they don't often refer to them as slides. You will find better results for a Google search using the term "watch glass". Due to the effects of outgassing of the mineral glass it is best that you try and purchase the thinnest slides possible. The substrate holder is designed to hold slides that are 1" or (25.4mm) in diameter.

Residual Gas Analyzer (RGA)

Replacement equipment & more detailed documentation can be found at www.thinksrs.com.

Description	Part No.	Cost
200 amu RGA	RGA200	\$4750.00
ThO2Ir Replacement Filament	O100RF	\$200.00
Replacement Ionizer Kit	O100RI	\$450.00

For additional help diagnosing problems see [http : //www.thinksrs.com/support/RGAsup.htm](http://www.thinksrs.com/support/RGAsup.htm). Also, the RGA pin diagram from ThinkSRS' website is available below.



RGA Pin Diagram

Crucibles & Heating Elements

The current basket and crucible combination was purchased from Kurt J. Lesker. A wide variety of other options are available from their website if you want to try something different.

Description	Part No.	Cost
Stranded Tungsten Basket	EVB8A3025W	\$34.00
Boron Nitride Crucible	EVC1BN	\$34.00

Notes: Kurt J. Lesker suggests that you only heat their stranded tungsten crucible to 1800°C . This is probably more of a precaution for the crucibles themselves rather than the tungsten. Additional information about many of the common materials used for crucibles is available at [http : //accuratus.com/materials.html](http://accuratus.com/materials.html).

Gas Leak Valve

This item was made by Varian, but was purchased from Ebay. Equivalent leak valves are sold by Kurt J. Lesker and other companies, but the cost is significantly greater than those sold on Ebay.

Description	Part No.	Cost
Varian Leak Valve	N/A	\$80.00

Appendix D

Equipment Troubleshooting & Repair

O-ring Construction Procedure

This step-by-step process describes the procedure used to construct a temporary O-ring for use with the 25" OD CF Flange of the vacuum chamber. Only Viton-A cord with a cross section of 0.108 in. should be used in the construction of this O-ring.

- First, as with any process involving a vacuum system, you should put on powder-free gloves.
- Take the old O-ring and cut it once so that it forms one long cord.
- Tape the old O-ring to a flat surface in a straight line. You may find the straight edge of a meter stick to be helpful in placing the cord in a straight line.
- Place the new cord stock next to the old O-ring with one end of the cord stock flush to one end of the old O-ring and tape it down if needed.
- Next, using the razor blade and a squaring tool, cut the cord stock perpendicular to the cord so that it is the same length as the old O-ring.
- Then perpendicularly cut a small amount of cord stock (about 1mm) off the other end of the newly cut Viton cord.
- At this point, in order to ensure a better bond between the cyanoacrylate and the Viton, both ends should be cleaned with isopropyl alcohol and allowed 15-20 minutes to dry.
- Once the alcohol has evaporated off of the Viton you will then place a small drop of cyanoacrylate on one end of the newly cut cord stock and the hold the ends together gently until the cyanoacrylate holds.
- Gently place the new O-ring in a safe location and let it cure for an hour or two before using.

This method will produce a stable O-ring capable of functioning properly under mild baking (less than 80°C) that should last long enough to order a new O-ring.

Appendix E

Vacuum Symbols [14]

All symbols with the exception of those marked with**) do not depend on the position.

**) These symbols may only be used in the position shown here (tip of the angle pointing down)

The symbols for vacuum pumps should always be arranged such that the side with the constriction is allocated to the higher pressure

Vacuum pumps







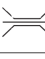
	Vacuum pump, general
	Piston vacuum pump
	Diaphragm vacuum pump
	Rotary positive displacement pump **
	Rotary plunger vacuum pump **
	Sliding vane rotary vacuum pump **
	Rotary piston vacuum pump **
	Liquid ring vacuum pump **
	Roots vacuum pump **
	Turbine vacuum pump, general
	Radial flow vacuum pump
	Axial flow vacuum pump
	Turbomolecular pump

	Ejector vacuum pump **
	Diffusion pump **
	Adsorption pump **
	Getter pump
	Sputter-ion pump
	Cryopump
	Scroll pump **
	Evaporation pump



Accessories

	Condensate trap, general
	Condensate trap with heat exchanger (e.g. cooled)
	Gas filter, general




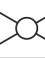

Table XVI: Symbols used in vacuum technology (extract from DIN 28401)






	Filtering apparatus, general
	Baffle, general
	Cooled baffle
	Cold trap, general
	Cold trap with coolant reservoir
	Sorption trap
	Throttling

Vacuum chambers







	Vacuum chamber
	Vacuum bell jar

Shut-off devices

	Shut-off device, general
	Shut-off valve, straight-through valve
	Right-angle valve
	Stop cock
	Three-way stop cock

	Right-angle stop cock
	Gate valve
	Butterfly valve
	Nonreturn valve
	Safety shut-off valve

Modes of operation

	Manual operation
	Variable leak valve
	Electromagnetic operation
	Hydraulic or pneumatic operation
	Electric motor drive
	Weight-operated

Connections and piping

















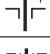

	Flange connection, general
	Bolted flange connection
	Small flange connection

Table XVI: Symbols used in vacuum technology (extract from DIN 28401) (continuation)

	Clamped flange connection
	Threaded tube connection
	Ball-and-socket joint
	Spigot-and-socket joint
	Taper ground joint connection
	Intersection of two lines with connection
	Intersection of two lines without connection
	Branch-off point
	Combination of ducts
	Flexible connection (e.g. bellows, flexible tubing)
	Linear-motion leadthrough, flange-mounted
	Linear-motion leadthrough, without flange
	Leadthrough for transmission of rotary and linear motion
	Rotary transmission leadthrough
	Electric current leadthrough

Measurement and gauges




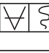
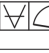
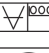

	General symbol for vacuum **)
	Vacuum measurement, vacuum gauge head **)
	Vacuum gauge, operating and display unit for vacuum gauge head **)
	Vacuum gauge, recording **)
	Vacuum gauge with analog measured-value display **)
	Vacuum gauge with digital measured-value display **)
	Measurement of throughput

Table XVI: Symbols used in vacuum technology (extract from DIN 28401) (continuation)

Appendix F

MATLAB Code for Analyzing Data

Rates.m

```
function [] = Rates()
clear; clc;
%Using the Vapor.m, Knudsen.m, and Temperature.m files this function
%calculates the appropriate reduced Chi-squared values for the data
%set.

%The column order should be as follows, pre-weight, post-weight,
%pressure, pressure uncertainty, current, voltage, and time elapsed
Data = xlsread('E:/Film Calculations/RateData.xlsx');
N = size(Data(1,:),2);

%Separating the data
Pre = Data(:,1);
Post = Data(:,2);
P = Data(:,3).*133.322368; %converting from Torr to Pa
P_u = Data(:,4).*133.322368;
C = Data(:,5);
V = Data(:,6);
Time = Data(:,7);

%Calculating theoretical values & uncertainties
[T,T_u] = Temperature(C,V);
[Pp,Pp_u] = Vapor(T,T_u);
[R,R_u] = Knudsen(T,T_u,Pp,Pp_u,P,P_u);

%Calculating actual values & uncertainties
[Rex,Rex_u] = Experimental(Pre,Post,Time);

Chi = sum(sum((R-Rex).^2)./(Rex_u.^2))
Chi_reduced = Chi/(N-1)
end
```

Temperature.m

```
function [T,T_u] = Temperature(C,V)
%The purpose of this function is to calculate the Temperature and its
%uncertainty for a black body with a given emissivity (eps). This is
%done using a combination of Joule's power relation for resistive
%heating and Ohm's law for resistors.

%This function assumes an uncertainty in the voltage and current of 0.1
%A/V respectively

sig = 5.67*10^(-8); %Stefan-Boltzmann constant
```

```

eps = 0.41; %emissivity of W between ~1700-2500 degree C
eps_u = 0.05; %the rough uncertainty of the emissivity
A = 0.00005141; %crucible surface area
A_u = 0.00000025; %uncertainty in the surface area
C_u = 0.1; %uncertainty in current
V_u = 0.1; %uncertainty in voltage

%There is a constant term in the partial derivative of T
dT_cons = (1/4)*(C.*V./(sig*eps*A)).^(-3/4);

%Calculating T
T = (C.*V./(sig*eps*A)).^(1/4);

%Calculating the uncertainty in T
T_u = sqrt( (C_u^2)*(dT_cons.*(V/(sig*eps*A))).^2 +... %current term
            (V_u^2)*(dT_cons.*(C/(sig*eps*A))).^2 +... %voltage term
            (eps_u^2)*(dT_cons.*(-C.*V/(sig*eps^2*A))).^2 +...
            %emissivity
            (A_u^2)*(dT_cons.*(-C.*V/(sig*eps*A^2))).^2); %area term

end

```

Vapor.m

```

function [Pp, Pp_u] = Vapor(T, T_u)
%This function is designed to calculate the experimental vapor pressure
%and its associated uncertainties due to heated Al at a given
%temperature as given by Wake Forest University's lab report.

%Calculate the partial pressure
Pp = 10.^((-15993./T) + 12.409 - 0.999*log10(T) - 3.52*10^(-6)*T);

%Calculate the uncertainty in the partial pressure
%If y = 10^x, then
%dy/dx = (10^x)*(ln 10)
Pp_u = sqrt((T_u.^2).*((Pp*log(10)).^2));

end

```

Knudsen.m

```

function [R, R_u] = Knudsen(T, T_u, Pp, Pp_u, P, P_u)
%This function calculates the deposition rate and its uncertainty using
%the angular independent form of the Langmuire-Knudsen relation.

Cm = 1.85*10^(-2); %a constant term
M = 26.9815386; %gram molecular mass of Al (courtesy of Wolfram Alpha)

```

```

r = 16.3; %source-substrate distance in cm
r_u = 0.5; %uncertainty in r

%Calculate R
R = Cm*sqrt(M./T).*(1/(r.^2)).*(Pp - P);

%Calculate the uncertainty in R
R_u = sqrt( (r_u^2)*(R.*(-2./r)).^2 +... %distance term
            (T_u.^2).*((1-2)*(M./(T.^2)).*(M./T).^(-1)).^2 +... %T term
            (P_u.^2).*(-Cm*sqrt(M./T).*(1/(r^2))).^2+... %P term
            (Pp_u.^2).*(Cm*sqrt(M./T).*(1/(r^2))).^2); %Pp term

end

```

Experimental.m

```

function [Rex,Rex_u] = Experimental(Pre,Post,Time)
%This function calculates the experimental deposition rates. This is
%done assuming the uncertainty in the deposition time to be constant,
%and accounting for slide outgassing by a constant adjustment factor in
%weight.

A = 2.68; %film surface area measure through scale projection method
(cm^2)
A_u = 0.08; %uncertainty in film surface area
out = 0.0012; %outgassing mass adjustment
Time_u = 1.5; %a generous uncertainty of 1.5 seconds
M_u = 0.0007; %uncertainty in the difference of mass measurement

%Calculating the difference in mass pre & post deposition
M = (Post + out) - Pre;

%Experimental rate calculation
Rex = M./(A.*Time);

%Experimental rate uncertainties
Rex_u = sqrt( (M_u^2)*(1./(A*Time)).^2 +... %mass term
            (Time_u^2)*(-1*(M./(A*Time.^2))).^2 +... %time term
            (A_u^2)*(-1*(M./(A^2*Time))).^2); %area term

end

```

Power Loss Calculator

This file should provide an approximate power lost during Joule heating on standard annealed copper wire. The purpose of which is to better estimate the power input provided by our power supply in order to better calculate the deposition rate of the material in our vacuum chamber.

Assumptions

For this calculation I'm assuming that the temperature of the wire doesn't change. The length of the wire is also assumed to be fixed (aka no thermal expansion). I'm also assuming that the gauge of the copper fixture inside the vacuum chamber is negligible. As of the moment, I'm also assuming that the resistivity of my wires per 1000 ft (values obtained from CRC F-114) is constant for both my 10 & 18 AWG wire.

R10 = 0.9989/304.8;

R18 = 6.385/304.8;

Length1 = 1;

Length2 = 0.7;

Current = 23.0;

Pow = 46.0;

Current^2*(R10*Length1 + R18*Length2)

%/Pow

This means that I'm losing almost 10 watts of power initially through my wires when I start it up. That is about 20% of my power lost through heat to the room. Lets see how much I lose when I add two more 18 AWG wires in parallel with my first 18 AWG wire. In this case though, I should note that my resistivity/meter coefficients are different (for this case I'll assume that the 18 gauge wire is hot ~75 degrees Celsius & the 10 gauge wire is still ~50 degrees Celsius).

R10 = 1.117/304.8;

R18 = 7.765/304.8;

Current = 39.0;

Pow = 237.9;

Current^2*(R10*Length1) + (1/3*Current)^2*(3*R18*Length2)

%/Pow

This means I'm losing roughly 14 watts at full power, which is roughly 6% of my total power input. Not a surprising amount, but I could use those extra 14 watts.

R[wlength_,rconst_] = rconst/304.8*wlength;

cmax = 42;

```
Manipulate[Plot[current^2 * R[l = Length, AWG10R] + (1 / Wires * current)^2 * (Wires * R[Length, AWG18R]),
  {current, 1, cmax}, AxesLabel -> {Input Current[A], Power Loss [W]}, Frame -> True, GridLines -> {{xpoint}, {ypoint}},
  GridLinesStyle -> Directive[Orange, Dashed]], {Wires, 1, 5, 1}, {Length, 0.1, 2}, {AWG10R, {0.9989, 1.117, 1.215}},
  {AWG18R, {6.385, 7.138, 7.765}}, {xpoint, 0, cmax, 0.1}, {ypoint, 0, 200, .01}]
```

